

Laser Diode Beam Shaping by Optical Interference

Takehiro FUKUSHIMA, Koichiro SAKAGUCHI, and Yasunori TOKUDA

Department of Communication Engineering, Faculty of Computer Science and System Engineering, Okayama Prefectural University, Soja, Okayama 719-1197, Japan

(Received December 2, 2010; Accepted February 23, 2011)

We recently proposed a novel beam shaping technique that employs Lloyd's mirror interference. In this study, we apply this technique to three commercial laser diodes: laser diodes used for optical pumping of solid-state lasers, for laser beam printers, and for laser displays. The elliptical output beams from these laser diodes could be transformed into nearly circular beams by inserting a mirror-polished GaAs substrate below the active layer of each laser diode and adjusting its height. The experimentally observed far-field patterns were predicted fairly well by numerical calculations based on Huygens' integral. We confirmed that our beam shaping technique is applicable to laser diodes with various wavelengths and vertical beam divergence angles. We also describe the monolithic configuration of the beam shaping system, which can be fabricated by dry etching. © 2011 The Japan Society of Applied Physics

Keywords: laser diodes, beam shaping, Lloyd's mirror interference, beam divergence angle, mirror-polished semiconductor substrate

1. Introduction

Laser diodes are often used as light sources in various scientific and engineering applications because of their compactness, low cost, and low power consumption.¹⁾ Many laser diode applications require a circular output beam. However, conventional laser diodes generate elliptical beams because light is confined in the waveguide differently in the horizontal and vertical directions.²⁾ Much effort has been expended in improving the output beam profiles of laser diodes. The most common methods involve optimizing the waveguide structure. These methods employ two different techniques to reduce the beam aspect ratio: reducing the vertical beam divergence by reducing the active layer thickness³⁾ and increasing the horizontal beam divergence by reducing the waveguide width.⁴⁾ However, both these techniques tend to degrade other specifications of the laser diode, such as the threshold current and the maximum output power. An alternative method is to introduce elements, such as conventional refractive optical elements,^{5–8)} graded-index optical elements,⁹⁾ micro-Fresnel lenses,¹⁰⁾ and holographic optical elements,¹¹⁾ to obtain collimated circular output beams. However, refractive optical elements containing anamorphic prism pairs are bulky and expensive. Although other optical elements are compact, they are difficult to fabricate and to align in an optical system. We recently proposed a simple and compact beam shaping technique that employs Lloyd's mirror interference.¹²⁾

In the present study, we apply this beam shaping technique to three typical laser diodes: laser diodes used for optical pumping of solid-state lasers, for laser beam printers, and for laser displays. The elliptical output beams from these laser diodes could be transformed into nearly circular output beams by inserting a mirror-polished GaAs substrate immediately below the active layer and adjusting its height. The experimentally observed far-field patterns were predicted fairly well by numerical calculations based on Huygens' integral. The tailored beam shape depends on

the height of the active layer above the mirror surface, the lasing wavelength, and the vertical beam divergence angle of the laser diode. The dependences of the tailored output beam shapes on these parameters are discussed. We also discuss the power concentration ratio of the first-order interference beam.

This paper is organized as follows. In §2, we briefly review the beam shaping technique using Lloyd's mirror interference. We also explain the numerical calculation method based on Huygens' integral for calculating the far-field patterns of the output beams. In §3, we present the experimental and numerical results for beam shaping of the three laser diodes. In §4, we discuss the dependences of the tailored beams on the height of the active layer, the lasing wavelength, and the vertical beam divergence angle; these dependences were obtained by numerical calculations. The power concentration ratio of the first-order beam is also discussed. Finally, the conclusions are given in §5.

2. Beam Shaping Technique and Numerical Calculation Model

Figure 1 schematically depicts the method for tailoring the beam profile. The vertical beam divergence angles θ_v of laser diodes are generally larger than their horizontal beam divergence angles θ_h because they employ flat optical waveguides with very different vertical and horizontal dimensions [see Fig. 1(a)]. In this paper, we define the beam divergence angles θ_v and θ_h as the full widths at half-maximum (FWHM) for the vertical and horizontal far-field patterns, respectively. When a semiconductor substrate with a mirror-polished surface is inserted at an appropriate distance below the active layer, a portion of the beam emitted from the active layer is reflected from the substrate surface. It then interferes with the light that propagates directly from the active layer, producing a highly directional beam with a reduced vertical divergence [see Fig. 1(b)]. This kind of interference is known as Lloyd's mirror interference. We define h as the height of the active layer

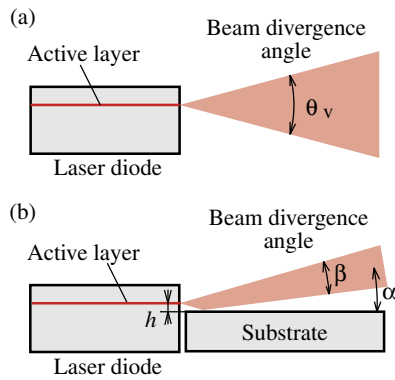


Fig. 1. (Color online) Cross-sectional view of laser diode in vertical direction: (a) without and (b) with substrate mirror.

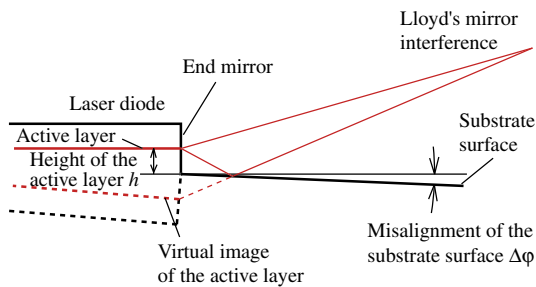


Fig. 2. (Color online) Numerical calculation model based on Huygens' integral.

above the substrate surface, as shown in Fig. 1(b). The direction angle α and the divergence angle β of the tailored beam can be controlled by adjusting the active layer height h . Here, α is defined as the angle at which the optical intensity is a maximum and β is defined as the FWHM of the vertical far-field pattern.

We next explain the numerical calculation method based on Huygens' integral. Figure 2 shows a schematic diagram of the numerical calculation model. We assumed that the near-field pattern of the laser diode is Gaussian in the calculations. This approximation is valid for our case because the observed far-field patterns are nearly Gaussian. The spot size ω_0 of the near-field pattern is estimated from the half-angle θ , which is estimated at the $1/e^2$ intensity point in the observed far-field pattern as¹³⁾

$$\omega_0 = \frac{\lambda}{\pi\theta}. \quad (1)$$

Here, λ is the lasing wavelength in vacuum. The far-field pattern was then calculated using Huygens' integral¹⁴⁾ of the near-field pattern. The reflection at the substrate surface was accounted for by calculating the virtual image of the active layer (see Fig. 2); this virtual image has a π phase shift due to reflection at the substrate surface. We also accounted for the misalignment $\Delta\varphi$ of the substrate surface so as to model the experiment conditions as closely as possible. $\Delta\varphi$ mainly affects the beam angle α of the tailored beam. In the calculation, we assumed that the substrate mirror is a perfect mirror at the lasing wavelength.

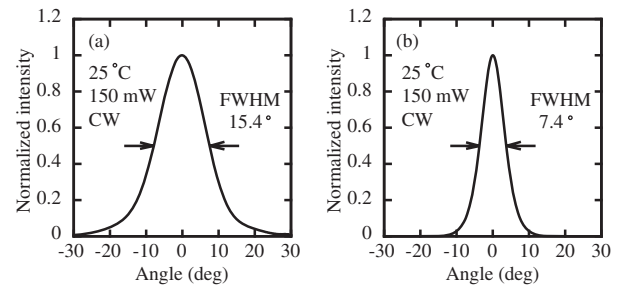


Fig. 3. Observed (a) vertical and (b) horizontal far-field patterns of laser diode for optical pumping.

3. Experimental and Numerical Results

In this section, we apply the beam shaping technique to the three laser diodes. The elliptical output beams emitted from laser diodes with different beam aspect ratios and wavelengths could be transformed into nearly circular beams by adjusting h .

3.1 Laser diode for optical pumping

We used a commercial infrared laser diode (Tottori Sanyo Electric DL-8141-035) in a TO-56 can package and a GaAs substrate with a mirror-polished surface. The window of the can package was removed and the stem of the package was partially removed by grinding so that the active layer could be accessed as close as possible. The laser diode was mounted on a heat sink and the substrate temperature of the laser diode was controlled at 25 °C using a temperature controller. The threshold current of the laser diode was measured to be 50.3 mA and its lasing wavelength was measured to be 809.1 nm at an output power of 150 mW. The GaAs substrate was installed on an *xyz*-translation stage that enabled the substrate to be positioned below the active layer of the laser diode. The height of the substrate was adjusted using the high-resolution motorized translation stage.

Figure 3 shows the far-field patterns of the laser diode at an output power of 150 mW without the GaAs substrate mirror. The optical intensity is normalized by the peak intensity and the origin of the horizontal axis corresponds to the angle at which the intensity is a maximum. The beam divergence angles θ_v and θ_h were measured to be 15.4 and 7.4°, respectively. Thus, the laser diode emitted an elliptical beam with an aspect ratio of 2.1.

The horizontal and vertical spot sizes ω_0 of the near-field pattern were respectively evaluated to be 2.15 and 1.06 μm from the far-field patterns shown in Fig. 3. Figure 4 shows the vertical far-field patterns obtained for four different values of h . To facilitate comparison, Fig. 4 is plotted with the same horizontal scale as Fig. 3(a). As h is increased, more higher-order beams appear in the vertical far-field pattern in addition to the first-order beam. In Fig. 4(a), the first-order beam, which has the highest intensity of all the beams, has a small beam divergence angle (2.1°). Its intensity is almost zero at angles less than 0° since this region is blocked by the GaAs substrate mirror. The misalignment angle $\Delta\varphi$ of the substrate mirror was

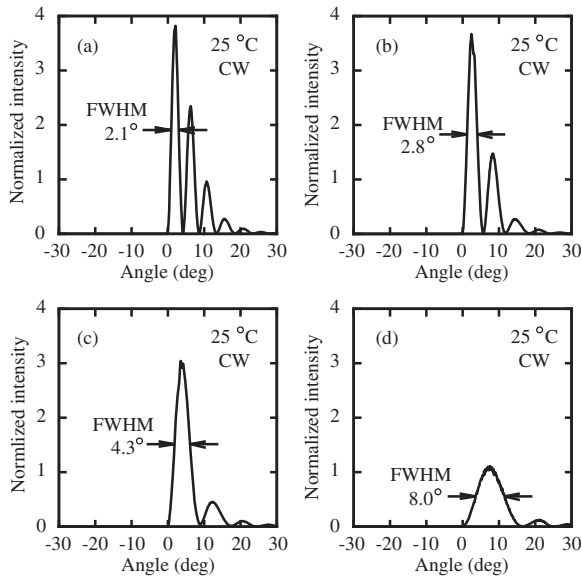


Fig. 4. Observed vertical far-field patterns for four different active layer heights h . h was gradually reduced from (a) to (d).

estimated to be 0° . As h is reduced, the number of beams in the vertical far-field pattern decreases and the divergence angle of the first-order beam increases [see Figs. 4(b) and 4(c)]; a nearly single-peak beam is obtained when h is sufficiently small [see Fig. 4(d)]. The vertical beam divergence angle β in Fig. 4(d) is estimated to be 8.0° .

Figure 5 shows the calculated far-field patterns corresponding to the experimental results in Figs. 4(a)–4(d). The intensity scale is normalized by the peak intensity of the far-field pattern calculated for the case without the substrate mirror. Since angles less than 0° are blocked by the GaAs mirror, we set the far-field intensity in this region to zero. In this calculation, the values of h were estimated by fitting the experimentally obtained far-field patterns with the numerically calculated ones so as to maximize the correlation coefficient. The values of h in the calculation that produce beam profiles that most closely correspond to the observed far-field patterns in Figs. 4(a)–4(d) are approximately 5.5, 4.1, 2.7, and $1.2\ \mu\text{m}$, respectively. The numerically calculated far-field patterns exhibit the same trends as the experimentally observed far-field patterns. Specifically, the number of interference beams in the vertical far-field pattern decreases and the vertical beam divergence angle of the first-order beam increases as h is reduced. On the other hand, some discrepancy between the observed far-field patterns and calculated far-field patterns was observed. In the case of a low h value, the peak intensity of the observed far-field pattern is smaller than that of the calculated one [see Figs. 4(d) and 5(d)]. It is conjectured that the optical loss due to the gap between the laser facet and the GaAs substrate causes the decrease in the peak intensity.

Figure 6 shows the dependences of the beam angle α and the beam divergence angle β of the first-order interference beam on the active layer height h . The open circles denote the experimental results and the solid line indicates the

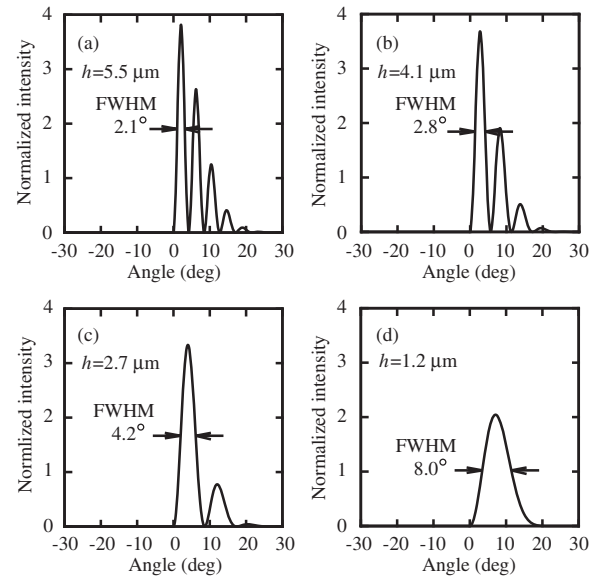


Fig. 5. Calculated vertical far-field patterns for active layer heights h of (a) 5.5, (b) 4.1, (c) 2.7, and (d) $1.2\ \mu\text{m}$.

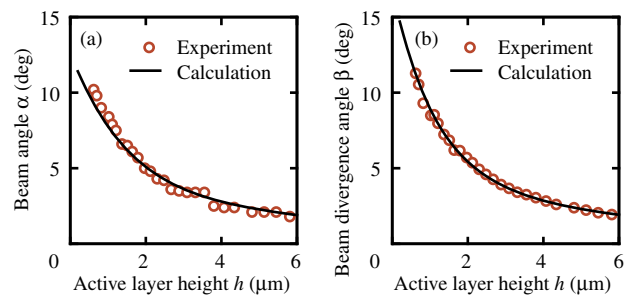


Fig. 6. (Color online) Relationships between active layer height and (a) beam angle and (b) beam divergence angle for laser diode designed for optical pumping.

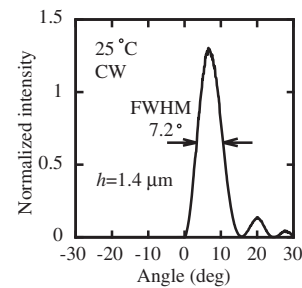


Fig. 7. Vertical far-field pattern for active layer height of $1.4\ \mu\text{m}$.

results of the numerical calculation using Huygens' integral. The experimental and numerical results exhibit good agreement. When h is relatively high, α and β are low; α and β increase as h is reduced. β is estimated to be 7.2° when $h = 1.4\ \mu\text{m}$ (see Fig. 7). The measured beam divergence angle β is close to the horizontal beam divergence angle θ_h of 7.4° [see Fig. 3(b)]. Thus, employing a GaAs substrate transformed the beam shape from elliptical to nearly circular.

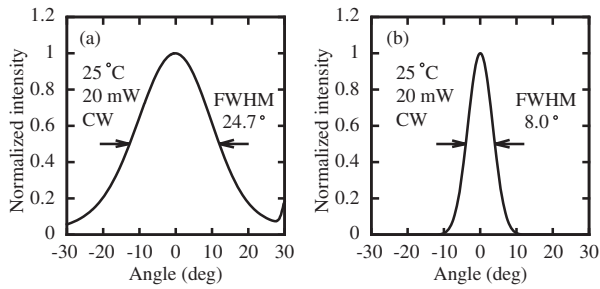


Fig. 8. Observed (a) vertical and (b) horizontal far-field patterns of laser diode for laser printers.

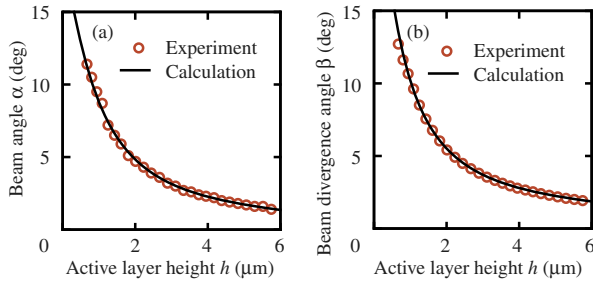


Fig. 9. (Color online) Relationships between active layer height and (a) beam angle and (b) beam divergence angle for laser diode designed for laser beam printers.

3.2 Laser diode for laser beam printers

We used a commercial infrared laser diode (Tottori Sanyo Electric DL-4140-001S) in a TO-56 can package. The laser diode has a larger vertical beam divergence angle but a smaller output power than the laser diode for optical pumping. The threshold current of the laser diode was measured to be 22.7 mA and its lasing wavelength was measured to be 783.3 nm at an output power of 20 mW. Figure 8 shows the far-field patterns of the laser diode at an output power of 20 mW without the GaAs mirror. The beam divergence angles θ_v and θ_h were measured to be 24.7 and 8.0°, respectively. Thus, the laser diode emits an elliptical beam with an aspect ratio of 3.1.

The spot size ω_0 of the near-field pattern was evaluated to be 0.63 μm in the vertical direction and 2.13 μm in the horizontal direction from the far-field patterns shown in Fig. 8. The far-field patterns with a GaAs substrate mirror exhibit similar trends as those for the laser diode for optical pumping. The misalignment angle $\Delta\varphi$ of the substrate mirror was estimated to be 0.5°. Figure 9 shows the dependences of the beam angle α and the beam divergence angle β of the first-order interference beam on the active layer height h . The open circles denote the experimental results and the solid lines indicate the numerical calculation results using Huygens' integral. The experimental and numerical results exhibit excellent agreement. α and β increase as h is reduced. β is estimated to be 8.5° when $h = 1.3 \mu\text{m}$ (see Fig. 10). The measured beam divergence angle β is close to the horizontal beam divergence angle θ_h of 8.0° [see Fig. 8(b)]. Thus, employing a GaAs substrate could transform the beam shape from elliptical to nearly circular.

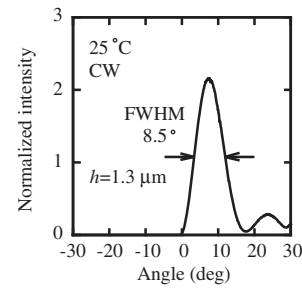


Fig. 10. Vertical far-field pattern for active layer height of 1.3 μm .

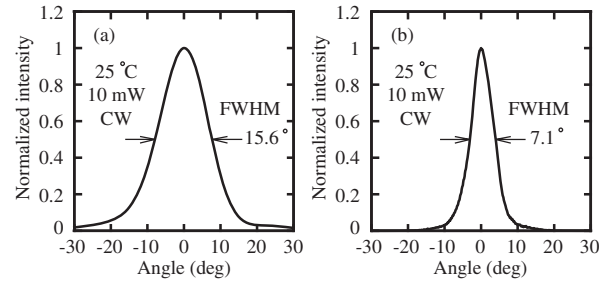


Fig. 11. Observed (a) vertical and (b) horizontal far-field patterns of laser diode for laser displays.

3.3 Laser diode for laser displays

In this experiment, we used a commercial visible laser diode (Tottori Sanyo Electric, DL-6148-030) in a TO-56 can package. The threshold current of the laser diode was measured to be 58.9 mA and its lasing wavelength was measured to be 642.4 nm at an output power of 10 mW. Figure 11 shows the far-field patterns of the laser diode at an output power of 10 mW without the GaAs mirror. The beam divergence angles θ_v and θ_h were measured to be 15.6 and 7.1°, respectively. Thus, the laser diode emits an elliptical beam with an aspect ratio of 2.2.

The spot size ω_0 of the near-field pattern was evaluated to be 0.84 μm in the vertical direction and 1.76 μm in the horizontal direction from the far-field patterns shown in Fig. 11. The far-field patterns with a GaAs substrate mirror exhibit similar trends as those for the laser diode for optical pumping. The misalignment angle $\Delta\varphi$ of the substrate mirror was estimated to be 2.3°. Figure 12 shows the dependences of the beam angle α and the beam divergence angle β of the first-order interference beam on the active layer height h . The open circles denote the experimental results and the solid lines indicate the results of numerical calculations using Huygens' integral. There is considerable discrepancy between the observed beam divergence angle and the numerical calculated beam divergence angle at low h , as shown in Fig. 12(b). We have not determined the reason for this discrepancy, but it is conjectured that the misalignment angle $\Delta\varphi$ of the substrate mirror may affect the discrepancy, because $\Delta\varphi$ is considerably larger than those in the experiments on the previous two laser diodes. α and β increase as h is reduced. β is estimated to be 7.0° when

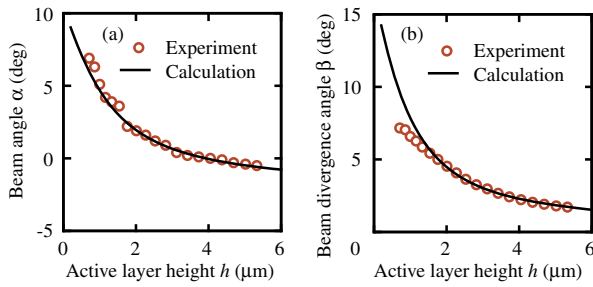


Fig. 12. (Color online) Relationships between active layer height and (a) beam angle and (b) beam divergence angle for laser diode designed for laser displays.

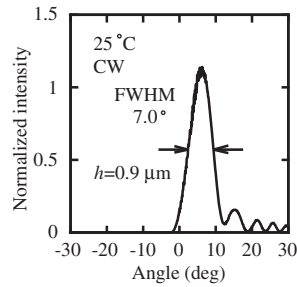


Fig. 13. Vertical far-field pattern for active layer height of 0.9 μm .

$h = 0.9 \mu\text{m}$ (see Fig. 13). The measured beam divergence angle is close to the horizontal beam divergence angle of 7.1° [see Fig. 11(b)]. Thus, employing a GaAs substrate transformed the beam shape from elliptical to nearly circular.

4. Discussion

In §3, we presented the experimental and numerical results for beam shaping of three laser diodes using Lloyd's mirror interference. The tailored beam shape strongly depends on the active layer height h , the lasing wavelength λ , and the vertical beam divergence angle θ_v . Below, on the basis of numerical calculations, we discuss the dependences of these parameters on the tailored beam shape. Figure 14 shows the dependence of the beam angle α and the beam divergence angle β on h for lasing wavelengths of 638 and 808 nm. In this calculation, the beam divergence angles θ_v and θ_h were set to be 16.0° and 8.0° , respectively. Both α and β increase as h decreases. Nearly circular beams were obtained when h was 0.9 and $1.2 \mu\text{m}$ for lasing wavelengths λ of 638 and 808 nm, respectively. The optimum value of h for obtaining a circular beam increased as λ increased.

Figures 15(a) and 15(b) respectively show the dependences of the beam angle α and the beam divergence angle β on h for various values of θ_v . In this calculation, λ was set to be 808 nm and the horizontal beam divergence angle θ_h was set to be 8.0° . Nearly circular beams were obtained when h was 0.9, 1.2, 1.3, and $1.4 \mu\text{m}$ for θ_v of 12.0° , 16.0° , 20.0° , and 24.0° , respectively. The optimum value of h for obtaining a circular beam increases as the vertical beam

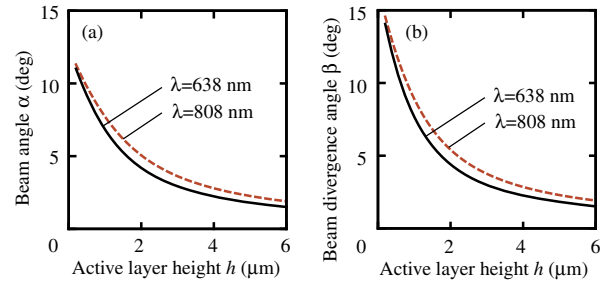


Fig. 14. (Color online) Calculated relationships between active layer height and (a) beam angle and (b) beam divergence angle for lasing wavelengths of 638 and 808 nm.

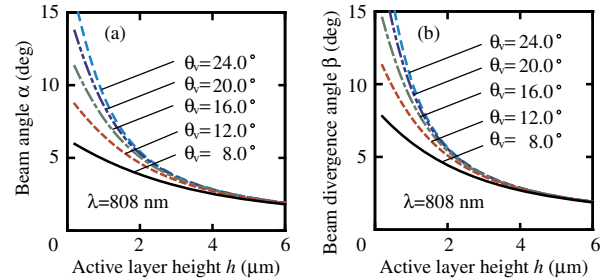


Fig. 15. (Color online) Calculated relationships between active layer height and (a) beam angle and (b) beam divergence angle for different vertical beam divergence angles of laser diode.

divergence angle θ_v increases. By adjusting h , a nearly circular beam can be obtained over a wide lasing wavelength range and over a wide range of the vertical beam divergence angle.

Next we discuss the power concentration ratio of the first-order beam in the total beams including higher-order beams for the far-field patterns. We estimated the power ratio by integrating the far-field intensity of the tailored beams shown in Fig. 5. It was estimated to be 46, 60, 81, and 100% for the h values of 5.5, 4.1, 2.7, and $1.2 \mu\text{m}$, respectively. When h is $5.5 \mu\text{m}$, considerable optical power is distributed to the higher-order beams, accordingly, the power ratio is relatively small. As h decreases, the number of higher-order beams decreases. As a result, the power ratio increases. In the case of $h = 1.2 \mu\text{m}$, higher-order beams disappear and the power ratio becomes 100%. Accordingly the beam shaping method using Lloyd's mirror interference is theoretically very efficient. Next we discuss the experimental results. The power concentration ratio is estimated to be 49, 65, 84, and 93% for the far-field patterns shown in Figs. 4(a)–4(d), respectively. As the height of the active layer decreases, the power ratio increases, similar to the calculation results. In the case of Fig. 4(d), 93% of the optical power is concentrated on the first-order beam. In the experiment, however, the total power of the far-field emission is attenuated compared with that without the substrate mirror. By integrating the far-field intensity shown in Figs. 4 and 3(a), the power attenuation is estimated to be 94, 92, 90, and 54% for the far-field patterns shown in Figs. 4(a)–4(d), respectively. We defined the power

attenuation as a ratio of the integrated far-field intensity of the tailored beam to that without substrate mirror. The power attenuation is attributed to the decrease in the peak intensity in the far-field pattern, as discussed in §3. It is important to determine the reason for the decrease in the peak intensity in the far-field pattern and to improve the power attenuation.

Finally, we mention the compactness of the beam shaping system. Advances in dry etching now permit highly vertical cavity end mirrors and a GaAs substrate mirror to be formed monolithically.¹⁵⁾ Thus, dry etching permits a compact beam shaping system to be fabricated simply. Conventional optical systems containing an anamorphic lens and cylindrical lens are bulky and expensive. The beam shaping system using Lloyd's mirror interference has the potential to miniaturize the optical system and lower the cost of optical systems.

In this study, we considered the far-field patterns of the tailored beams. However, it should be noted that a circular beam does not necessarily guarantee good beam quality. We intend to evaluate the beam quality of the tailored optical beam in a future study.

5. Conclusions

We applied a beam shaping technique using Lloyd's mirror interference to three commercial laser diodes with different lasing wavelengths and vertical beam divergence angles. The elliptical output beams from the laser diodes could be transformed to nearly circular output beams by inserting a mirror-polished GaAs substrate immediately below the active layer and adjusting the height of the GaAs substrate mirror. The experimentally observed far-field patterns were predicted fairly well by numerical calculations using Huygens' integral. The numerical calculations predict that a nearly circular beam can be obtained over a wide wavelength range and a wide range of the vertical beam

divergence angle by adjusting the height of the active layer. The beam shaping system can be monolithically fabricated by dry etching.

Acknowledgment

This work was supported in part by a Grant-in-Aid for Scientific Research C from the Japan Society for the Promotion of Science.

References

- 1) T. Suhara: *Semiconductor Laser Fundamentals* (Merzel Dekker, New York, 2004) Sect. 1.4, p. 14.
- 2) X. Zeng and A. Naqwi: *Appl. Opt.* **32** (1993) 4491.
- 3) H. C. Casey, Jr. and M. B. Panish: *Heterostructure Lasers* (Academic Press, New York, 1978) Sect. 2.7, p. 71.
- 4) A. Furuya, T. Fukushima, Y. Kito, C. Anayama, M. Sugano, H. Sudo, M. Kondo, and T. Tanahashi: *Electron. Lett.* **30** (1994) 416.
- 5) J. F. Forkner and D. W. Kuntz: *Proc. SPIE* **740** (1987) 27.
- 6) Y. Adachi: *Proc. SPIE* **740** (1987) 36.
- 7) K. Otsuka, K. Abe, J.-Y. Ko, and T.-S. Lim: *Opt. Lett.* **27** (2002) 1339.
- 8) M. Kuznetsov, F. Hakimi, R. Sprague, and A. Mooradian: *IEEE J. Sel. Top. Quantum Electron.* **5** (1999) 561.
- 9) S. Sinzinger, K.-H. Brenner, J. Moisel, T. Spick, and M. Testorf: *Appl. Opt.* **34** (1995) 6626.
- 10) S. Ogata and Y. Ito: *Opt. Eng.* **33** (1994) 3656.
- 11) A. Aharoni, J. W. Goodman, and Y. Amitai: *Opt. Lett.* **18** (1993) 179.
- 12) T. Fukushima, K. Miyahara, and N. Nakata: *IEICE Trans. Electron.* **E92-C** (2009) 1095.
- 13) A. E. Siegman: *Lasers* (University Science Books, Mill Valley, CA, 1986) Chap. 17, p. 663.
- 14) A. E. Siegman: *Lasers* (University Science Books, Mill Valley, CA, 1986) Chap. 16, p. 626.
- 15) T. Fukushima, T. Harayama, T. Miyasaka, and P. O. Vaccaro: *J. Opt. Soc. Am. B* **21** (2004) 935.